Electronic Supplementary Information

"Self-healing and mechanical performance of dynamic glycol chitosan hydrogel nanocomposites"

Spyridon Efstathiou,[a] Alan M. Wemyss,[a,b] Georgios Patias,[a] Lucas Al-Shok,[a] Maria Grypioti,[a] Despina Coursari,[a] Congkai Ma,[a] Christophe J. Atkins,[a] Ataulla Shegiwal,[a] Chaoying Wan,[b] and David M. Haddleton [a]*

[α] Department of Chemistry, University of Warwick, Gibbet Hill Road, CV4 7AL, Coventry, UK

[b] International Institute for Nanocomposites Manufacturing (IINM), WMG, University of Warwick, CV4 7AL, UK

Contents

Experimental Section

Materials

N, N-Dimethyl acrylamide (DMAc, 97%) and *N*-hydroxyethyl acrylamide (HEAm, 97%) were purchased from Sigma-Aldrich and purified by passing through a column of activated basic alumina (Sigma-Aldrich) to remove inhibitors prior use. Poly(ethylene glycol) ($PEG_{2,000}$, M_n = 2,000 g.mol^{-1}, BioUltra), Poly(ethylene glycol) ($PEG_{4,000}$, M_n = 4,000 g.mol^{-1}, Sigma-Aldrich), triethylamine (TEA, ≥99%), α-bromoisobutyryl bromide (BIBB, 98%), 4-(dimethylamino)pyridine (DMAP, ReagentPlus®, ≥99%), 4-formyl benzoic acid (FBA, 97%), ninhydrin (99%) and glycol chitosan (GC, ≥ 60%(titration), crystalline) were all purchased from Sigma-Aldrich and used directly unless otherwise stated. *N, N'*-Dicyclohexylcarmodiimide (DCC, 99%, Alfa Aesar by Thermo Fisher Scientific) and D-glucosamine HCl (BIOSYNTH® Carbosynth) were also used as received. HPLC graded water (H_2O, VWR international, LLC) was used as the solvent for disproportionation and polymerizations. *Tris*(2-(dimethylamino)ethyl)amine (Me_6TREN) was synthesized according to previous reported literature procedures.[1] Copper(I) bromide (Cu(I)Br, 98%, Sigma-Aldrich) was sequentially washed with acetic acid and ethanol and dried under vacuum. Dialysis membranes (MWCO = 1 kDa and 3.5 kDa) were purchased from Specta/Por®. Graphene oxide (GO, 97-98%; Abalonyx) was used as received.

Characterization Techniques

Size exclusion chromatography (SEC) analysis was performed on an Agilent PL-50 instrument equipped with differential refractive index (DRI) and dual ultraviolet (UV) detectors set to λ = 250 nm. The mobile phase used was DMF + 0.1% LiBr at 50 °C at a flow rate of 1.0 mL min^{-1} (poly(methyl methacrylate) (PMMA) standards (Agilent EasyVials) were used for calibration). The system was equipped with 2 x PolarGel Mixed C columns (300 x 7.5 mm) and a PLgel 5.0 μm guard column. Polymers were dissolved in DMF and filtered through a GVHP nylon membrane (0.22 μm pore size) prior analysis. Experimental molar mass ($M_{n,SEC}$) and dispersities ($Đ_M$) were determined using Agilent GPC/SEC software.

^{1}H-NMR, ^{13}C-NMR and DOSY-NMR spectra were recorded on a Bruker DPX-400 or a Bruker DPX-500 MH_z instrument, using deuterated chloroform ($CDCl_3$) or deuterated dimethyl sulfoxide (DMSO-d_6) as solvents. Chemical shifts are given as δ in parts per million (ppm) downfield from the internal standard tetramethylsilane (TMS) at δ = 0 ppm. For

polymerization kinetics, ^{1}H-NMR spectra were recorded in DMSO-d_6 using acetonitrile (δ = 2.07 ppm) as an internal reference. All spectra were analyzed using ACD/NMR Processor software.

Infrared spectra were recorded using a Bruker ALPHA II Fourier transform infrared (FTIR) spectrometer.

Matrix assisted laser desorption/ionization-time of flight mass spectrometry (MALDI-ToF MS) was performed on a Bruker Daltonics Ultra flex II MALDI-ToF-MS mass spectrometer, equipped with a nitrogen laser delivering 2 ns laser pulses at 337 nm with positive ion ToF detection performed using an accelerating voltage of 25 kV. Solutions were prepared as following: *trans*-2-[3-(4-*tert*-Butylphenyl)-2-methyl-2-propenylidene] malononitrile (DCTB) as a matrix (20 µL) and sample (10 mg mL^{-1}) were initially mixed and 0.5 µL of the mixture was applied on the target plate. Spectra recording was made in linear mode calibrating with either PEG-Me 1,900-5,000 Da or PEG 4,000 Da.

Thermogravimetric analysis (TGA) was carried out on a Mettler Toledo TGA1/DSC1-STAR^{e} instrument under nitrogen flow (50 mL min^{-1}) at a heating rate of 10 ^{o}C min^{-1}. Samples were heated from 0 ^{o}C up to 600 ^{o}C in 40 µL aluminium pans. The decomposition temperature (T_{deg}) was defined as the temperature of 50% loss of the total weight for all curves.

Rheological analysis was performed in an Anton Paar MCR 302 rheometer equipped with a parallel plate configuration (25 mm diameter). The data was analyzed using RheoCompass software.

Compression tests were carried out using a Shimadzu EZ-LX Universal Testing Instrument equipped with a 50 N load cell.

UV-Vis spectra were recorded on an Agilent Technologies Cary 60 UV-Vis spectrometer in the range of 200-1100 nm using HPLC graded water as a solvent. For all measurements a glass cuvette (purchased from HELLMA) with a 10 mm optical length was used.

Raman spectroscopy was performed on a Renishaw inVia Reflex Raman Microscope spectrometer using a 532 nm DPSS laser source.

Transmission Electron Microscopy (TEM) images were obtained using a Jeol 2100 TEM, operated at 200 kV and fitted with a Gatan Ultrascan 1000 camera. Samples for TEM analysis were prepared *via* drop-casting a few milliliters of sample dispersions after ultrasonication onto holey carbon grids, allowing the solvent to evaporate and leaving the sample to rest for 24 hours at ambient temperature.

Synthetic Procedures

Synthesis of poly(ethylene glycol) bis (2-bromoisobutyrate) initiator.

$PEG_{2,000}$ (30.0 g, 15 mmol, 1 eq.) was charged in a round bottom flask equipped with a magnetic stirring bar and left degas under nitrogen for 30 min. Anhydrous DCM (300 mL) was cannulated into the flask and the mixture was stirred for 5 min. TEA (6.3 mL, 3 eq.) was added to the solution *via* a deoxygenated syringe and the mixture was placed in an ice bath. BIBB (5.6 mL, 3 eq.) was added dropwise for a total of 30 min using a syringe pump. Upon complete addition, the mixture was left to stir at 0 °C for 30 min and at ambient temperature overnight. Filtration was followed to remove the amine salt and the organic phase was washed with a saturated solution of Na_2CO_3 (4 × 100 mL). The organic phase was dried over $MgSO_4$ before the volatiles were removed *in vacuo* to yield a light-yellow liquid. The solid was dissolved in the minimum amount of THF and precipitated twice in cold petroleum ether (60-80 °C) to afford a yellow solid (25 g, 83.3%).

^{1}H-NMR (400 MHz, $CDCl_3$), δ (ppm): 4.26 (t, 4H, J_1 = 9.7 Hz, J_2 = 4.9 Hz, CO-O-C**H**$_2$-CH_2), 3.75 (t, 4H, J_1 = 9.7 Hz, J_2 = 5.1 Hz, CO-O-CH_2-C**H**$_2$), 3.58 (s, 176H, -O-C**H**$_2$-C**H**$_2$) and 1.87 (s, 12H, - (C**H**$_3$)$_2$).

^{13}C-NMR (400 MHz, $CDCl_3$), δ (ppm): 30.7, 65.1, 68.7 and 70.5.

FT-IR (ν, cm^{-1}): 3,000 (C-H stretch), 1,750 (O-CO-R), 1,380 (-$(CH_3)_2$), 1,300 (CH stretch), 1,200 (CH stretch).

$\boldsymbol{M}_{\mathbf{n,\,MALDI}}$ = 2,318.015 Da, calculated for $[C_{98}H_{192}Br_2O_{48}+Na]^+$ = 2,318.085 Da

$\boldsymbol{M}_{\mathbf{n,\,SEC}}$ = 8,500 g.mol^{-1} ($\boldsymbol{Đ}$ = 1.04)

Synthesis of ABA telechelic copolymer by aqueous Cu-RDRP targeting a DP_n = 80 at a molar ratio of (DMAc:HEAm) = (88:12) .

Synthesized bifunctional initiator (M_n = 2,300 g.mol^{-1}, 1.38 g), H_2O (28 mL), DMAc (4.13 mL, 0.04 mol) and HEAm (0.6 mL, 5.7 mmol) were charged in a round bottom flask. The flask was

fitted with a rubber septum and degassed with nitrogen for 15 min. Cu(I)Br (34.4 mg, 0.4 eq. with respect to the initiator), H_2O (2 mL) and a magnetic stir bar were charged to a second round bottom flask, immersed in an ice bath, and degassed for 5 min. Me_6TREN (64 µL, 0.4 eq. with respect to the initiator) was then added with rapid stirring to induce Cu (I) disproportionation leading to a blue solution with visible Cu (0) particles. Subsequently, after 1 min allowed for disproportionation, the deoxygenated mixture of the first flask was quickly transferred *via* a degassed syringe into the disproportionation mixture and polymerization was allowed to proceed at 0 °C for 30 min (>95% conv. by ^{1}H-NMR). Finally, polymers were dialyzed against water (MWCO = 1 kDa dialysis membrane) to remove remaining copper catalyst and unreacted substances following freeze drying to yield the final purified polymer **p(DMAc$_x$-*co*-HEAm$_y$)-*b*-PEG$_{2,000}$-*b*-p(DMAc$_x$-*co*-HEAm$_y$)** as a white powder. Polymers were analyzed by SEC and NMR.

$M_{n,\,SEC}$ = 17,800 g.mol^{-1} ($Đ$ = 1.18)
$M_{n,\,NMR}$ = 9,800 g.mol^{-1}

Synthesis of telechelic crosslinker *via* esterification of hydroxyl groups.

p(DMAc$_x$-*co*-HEAm$_y$)-*b*-PEG$_{2,000}$-*b*-p(DMAc$_x$-*co*-HEAm$_y$) (4.0 g, $n_{pol.}$ = 0.4 mmol, $M_{n,\,NMR}$ = 9,800 g.mol^{-1}, $Đ_M$ = 1.18, n_{-OH} = 3.6 mmol, molar ratio = 88:12, 1 eq.) was initially dissolved in 100 mL of toluene and the residual moisture was removed by azeotropic distillation to a volume of ~20 mL. Anhydrous dichloromethane (DCM, 50 mL) was then added and the solution was transferred to a two neck round bottom flask immersed in an ice bath. Following the indicated order, DMAP (0.4 g, 3.6 mmol, 1 eq.), DCC (3.7 g, 18 mmol, 5 eq.) and FBA (2.2 g, 14 mmol, 4 eq.) were added successively and the reaction mixture was left to react for 48 h under nitrogen at room temperature. The mixture was then filtered to remove insoluble substances and concentrated to a lower volume following precipitation (2×) in cold diethyl ether. The product was dried under vacuum for 24 h and the remaining powder was dissolved in water and centrifuged for 30 min to remove further insoluble impurities. The supernatant was collected and dialyzed against water (MWCO = 3.5 kDa dialysis membrane) and finally lyophilized to obtain the final post-modified crosslinker **p(DMAc$_x$-*co*-CHO$_y$)-*b*-PEG$_{2,000}$-*b*-p(DMAc$_x$-*co*-CHO$_y$)** as a yellow solid (85% yield). The modification efficiency was found to be above 99% by ^{1}H-NMR (500 MHz, DMSO-d$_6$) spectroscopy due to the complete disappearance of the –O**H** peaks at δ = 4.54-4.86 ppm.

$M_{n,\,SEC}$ = 21,600 g.mol^{-1} ($Đ$ = 1.25)

$M_{n,\,NMR}$ = 11,600 g.mol^{-1}

Synthesis of bifunctional $PEG_{4,000}$ crosslinker (Bi-$PEG_{4,000}$) *via* esterification of the terminal hydroxyl groups.

$PEG_{4,000}$ (20.0 g, 5 mmol, 1 eq.) was mixed with 200 mL of anhydrous THF forming a white suspension. The flask was immersed in an ice-bath and DMAP (0.6 g, 5.0 mmol, 1 eq.), DCC (5.2 g, 25 mmol, 5 eq.) and FBA (3.0 g, 20 mmol, 4 eq.) were added successively and the reaction mixture was let react for 48 h under nitrogen at room temperature. The mixture was then filtered to remove insoluble substances and concentrated to a lower volume following precipitation (3×) in cold diethyl ether. The product was dried under vacuum for 24 h and the remaining powder was dissolved in water and centrifuged for 30 min to remove further insoluble impurities. The supernatant was collected and lyophilized to obtain the final bifunctional crosslinker Bi-$PEG_{4,000}$ as a white solid (87% yield). Modification efficiency was found to be above 99% by ^{1}H-NMR (400 MHz, $CDCl_3$) spectroscopy due to the complete disappearance of the –O**H** peaks at δ = 2.79 ppm .

$M_{n,\,SEC}$ = 21,600 g.mol^{-1} ($Đ$ = 1.25)

$M_{n,\,NMR}$ = 11,600 g.mol^{-1}

Ninhydrin assay for the quantification of amine groups in glycol chitosan.

The protocol was adapted from literature with slight modifications.[2] Initially, a six point standard curve of D-glucosamine HCl was obtained monitoring the maximum absorbance peak at λ_{max} = 570 nm. Firstly, 8.0 mg mL^{-1} of D-glucosamine HCl in HPLC graded water and 0.3 M of ninhydrin in ethanol were prepared and mixed to give six aliquots of 2 mL as shown in Table S1. Each aliquot was then transferred in a boiling water bath and left for 10 min (a sudden colour change to purple was noticed). All solutions were left to cool and their maximum absorbance was monitored to give the D-glucosamine HCl calibration curve. Similarly, four different concentrations of glycol chitosan solutions were prepared (1.6 mg mL^{-1}, 2.4 mg mL^{-1}, 3.2 mg mL^{-1} and 4.0 mg mL^{-1}) and their absorbance at λ_{max} = 570 nm was matched with the D-glucosamine HCl calibration curve to determine the moles of NH_2 groups / g of glycol chitosan.

Table S1. Detailed quantities used for ninhydrin assay.

D-glucosamine (8.0 mg mL^{-1}) (mL)	**H_2O (mL)**	**Ninhydrin (0.3 M) (mL)**	**D-glucosamine (mg mL^{-1})**	**[NH_2] (M)**
0.2	1.7	0.1	0.8	0.00447
0.4	1.5	0.1	1.6	0.00890
0.5	1.4	0.1	2.0	0.0112
0.6	1.3	0.1	2.4	0.0133
0.8	1.1	0.1	3.2	0.0179
1.0	0.9	0.1	4.0	0.0223

Hydrogels fabrication

Preparation of glycol chitosan/ crosslinker hydrogels.

Generally, hydrogels were formed using various molar ratios (-CHO/-NH_2) to examine their mechanical and self-healing properties. Briefly, in 500 μL of prepared glycol chitosan solution A, a chosen amount of polymer crosslinker (telechelic or Bi-$PEG_{4,000}$) solution B was added following proper mixing to form the hydrogels within certain time depicted from the chosen moles of crosslinker. By altering the volumes of the two solutions, hydrogels could be scaled up and down as needed.

[Solution A]: 3.0 wt % solution of glycol chitosan in PBS pH = 7.4
[Solution B]: 5.0 wt % solution of crosslinker (telechelic or Bi-$PEG_{4,000}$) in PBS pH = 7.4

Preparation and characterization of glycol chitosan/graphene oxide (GC/GOy) mixtures.

Dispersions of graphene oxide in PBS pH = 7.4 were prepared at 0.5 and 2.0 wt %. After excessive sonication for 30 min, the same mixtures were used to make up 3.0 wt % solutions of glycol chitosan/graphene oxide reported as GC/GO**(0.5)** and GC/GO**(2.0)**. Each GC/GO**(y)** mixture was stirred at 37 ^oC for 3 days (72 h) and further used for the preparation of nanocomposite hydrogels.

For characterisation purposes, the GC/GO**(y)** nanocomposites were isolated from the mixtures after centrifugation and repeated washings with distilled water to remove unreacted glycol chitosan. Finally, solids were dried in an oven at 50 ^oC and characterized *via* UV-Vis, FT-IR, Raman and TGA.

Preparation of glycol chitosan/ telechelic crosslinker nanocomposite hydrogels GC/TXL(x)-GO(y).

A similar protocol with the preparation of glycol chitosan/crosslinker hydrogels was followed. Briefly, in 500 μL of prepared GC/GO**(0.5)** or GC/GO**(2.0)** solution C, a chosen amount of polymer crosslinker solution B was added following proper mixing to form the hydrogels. By altering the volumes of the two solutions, the hydrogels could be scaled up and down as needed.

[Solution C]: 3.0 wt % solution of glycol chitosan/graphene oxide mixture (contain 5.0 wt % or 2.0 wt % GO) in PBS pH = 7.4

[Solution D]: 5.0 wt % solution of telechelic polymer crosslinker in PBS pH = 7.4

Hydrogel Characterization

Rheological Testing

All rheological characterization was performed on an Anton Parr MCR 302 rheometer with a measuring parallel plate (diameter of 25 mm) at 25 ^{o}C. For all gelation kinetic experiments, 200 μL of 3.0 wt % glycol chitosan solution or any GC/GO**(y)** mixture was spread on the parallel plate following addition of polymer crosslinker at predetermined molar ratios with respect to glycol chitosan. The upper plate was immediately lowered to give a 0.5 mm gap and the measurements conducted at a frequency of ω = 10 rad s^{-1} and a strain of γ = 1.0%. The evolution of gelation was monitored by time and the gel point was determined by the crossover point between the G' and G''. For all oscillatory sweep experiments, preformed hydrogel discs (diameter: 20 mm, height: 1.7 mm) were used after 2 h of curing to ensure complete gelation. Amplitude sweep measurements were carried out at a strain range of 0.01 to 500% using a constant angular frequency of ω = 10 rad s^{-1}. Frequency sweeps were conducted at an angular frequency, ω, range of 0.1 to 100 rad s^{-1} using a constant strain of 5.0%. All measurements were performed at least three times using distinct samples while results and statistical analysis was performed as an average of the total runs. All self-healing properties were also assessed by rheology by altering from low 1.0% to high 350% strain at a constant angular frequency of 10 rad s^{-1} for a total of seven cycles. Self-healing tests were performed at least twice using distinct samples for every run.

Compression Testing

All compression measurements were performed in a Shimadzu EZ-LX Universal Testing Instrument equipped with a 50 N load cell. Cylindrical shape hydrogels were prepared in glass vials of 2 mL with a diameter of 1.6 cm and height of 1.9 cm. Hydrogels were left to cure for 2 h in order to ensure complete formation of the hydrogel networks. A preload force of 0.01 N was set with a compression velocity set at 5 mm min^{-1}. All compression tests were repeated at least 8 times and the average was calcualated to determine the ultimate stress and strain at break (%). Compression modulus was calculated from the 10% of the stress/strain curve which was defined as:

$$\text{Modulus} = \frac{Difference\ in\ Stress}{Difference\ in\ Strain} \qquad (1)$$

For the compression tests of the self-healed hydrogels, materials were cut in half and recombined overnight. Then compression testing was performed in replicates and the self-healing efficiency was defined as:

$$\text{SH\%} = \frac{Modulus\ of\ self-healed\ material}{Modulus\ before\ self-healing} \times 100 \qquad (2)$$

Disk diffusion assay

For the disk diffusion experiments, bacterial strains of E. coli (K12 MG 1655) were stored at -80^{o}C. Fresh aliquots were subcultured on Nutrient agar and incubated at 35 ^{o}C for 24 h prior each experiment. Hydrogel nanocomposites were casted in small disk (based on the standard procedure) and applied on the surface of the agar plates to dry at room temperature for 20 min. The agar plates were then incubated at 37 ^{o}C for 24 h.

Supplementary data for $PEG_{2,000}$ bifunctional initiator synthesis

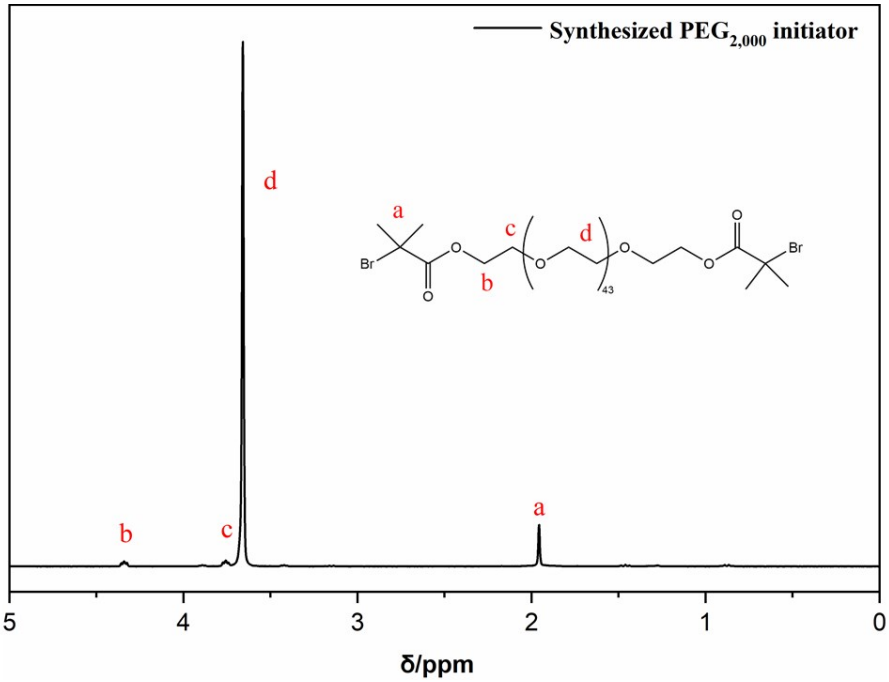

Figure S1. ^{1}H-NMR (400 MHz, CDCl3) spectrum of the bifunctional $PEG_{2,000}$ initiator.

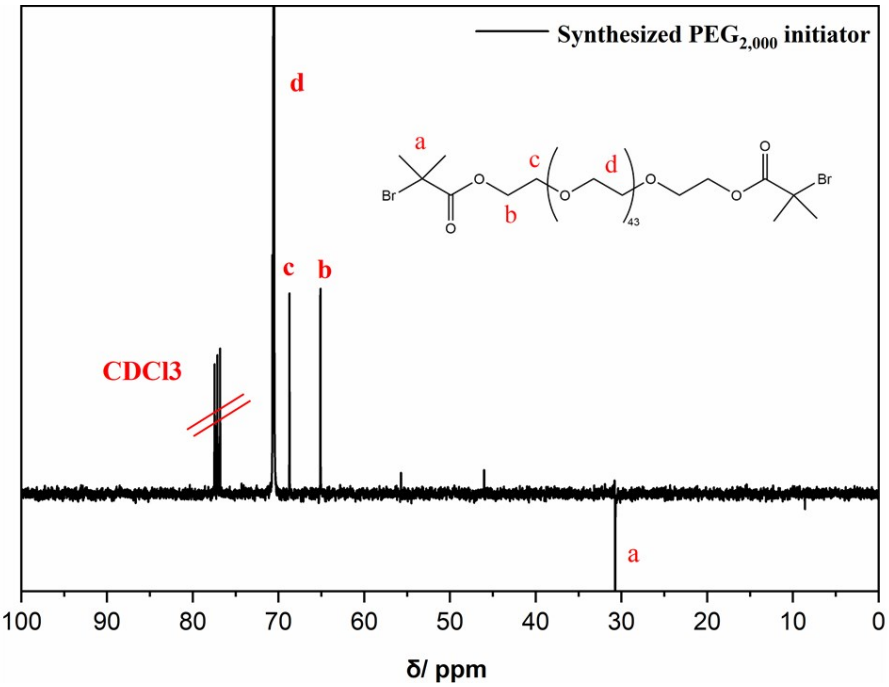

Figure S2. ^{13}C-NMR (400 MHz, CDCl3) spectrum of the bifunctional $PEG_{2,000}$ initiator.

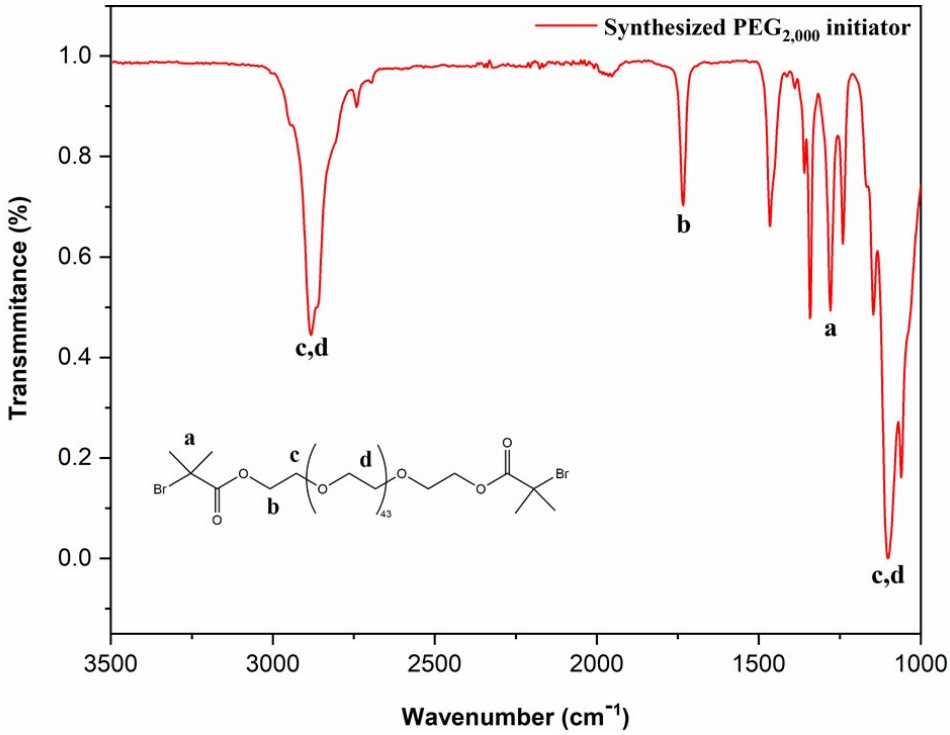

Figure S3. FT-IR spectrum of the bifunctional $PEG_{2,000}$ initiator.

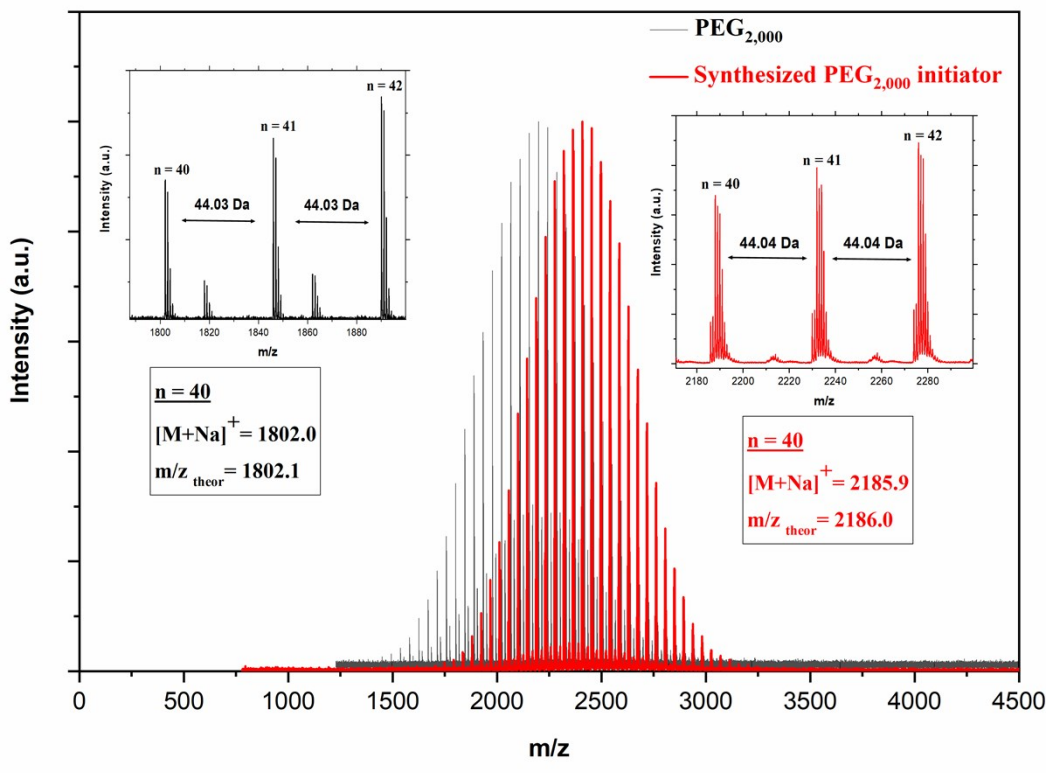

Figure S4. MALDI-ToF spectra comparison of $PEG_{2,000}$ and bifunctional $PEG_{2,000}$ initiator.

Supplementary data from the synthesis of the telechelic random copolymer p(DMAc$_x$-*co*-HEAm$_y$)-*b*-PEG$_{2,000}$-*b*-p(DMAc$_x$-*co*-HEAm$_y$)

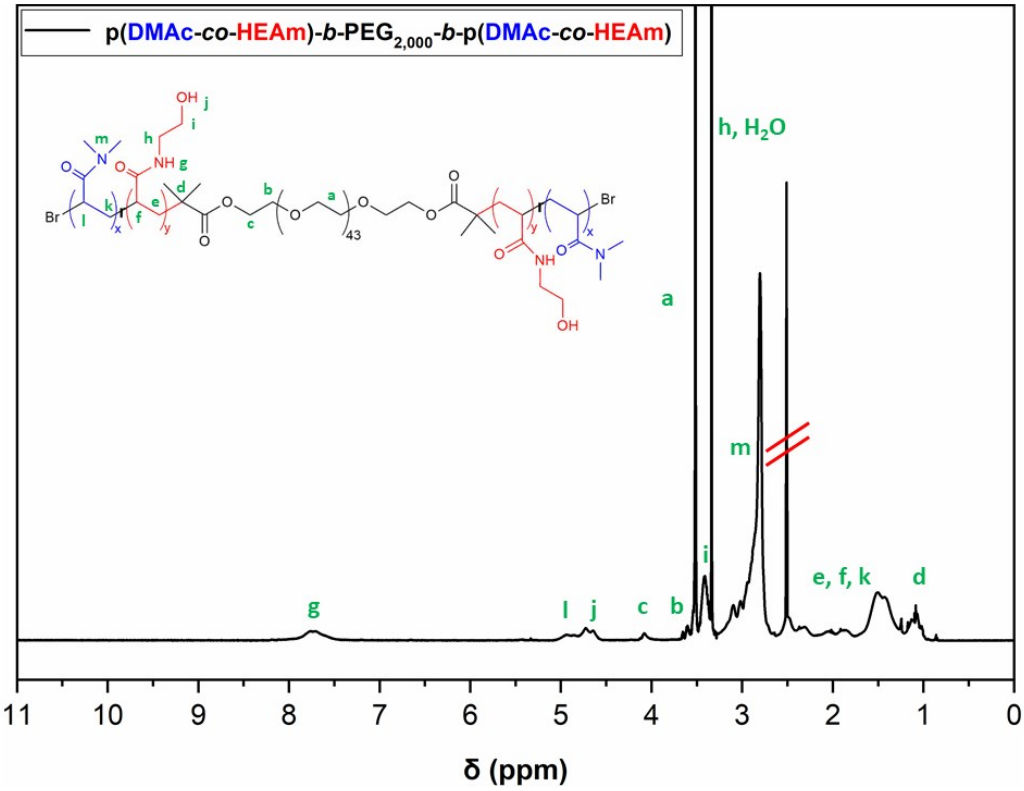

Figure S5. ^{1}H-NMR (400 MHz, DMSO-d$_6$) spectrum of p(DMAc$_x$-*co*-HEAm$_y$)-*b*-PEG$_{2,000}$-*b*-p(DMAc$_x$-*co*-HEAm$_y$) telechelic random copolymer.

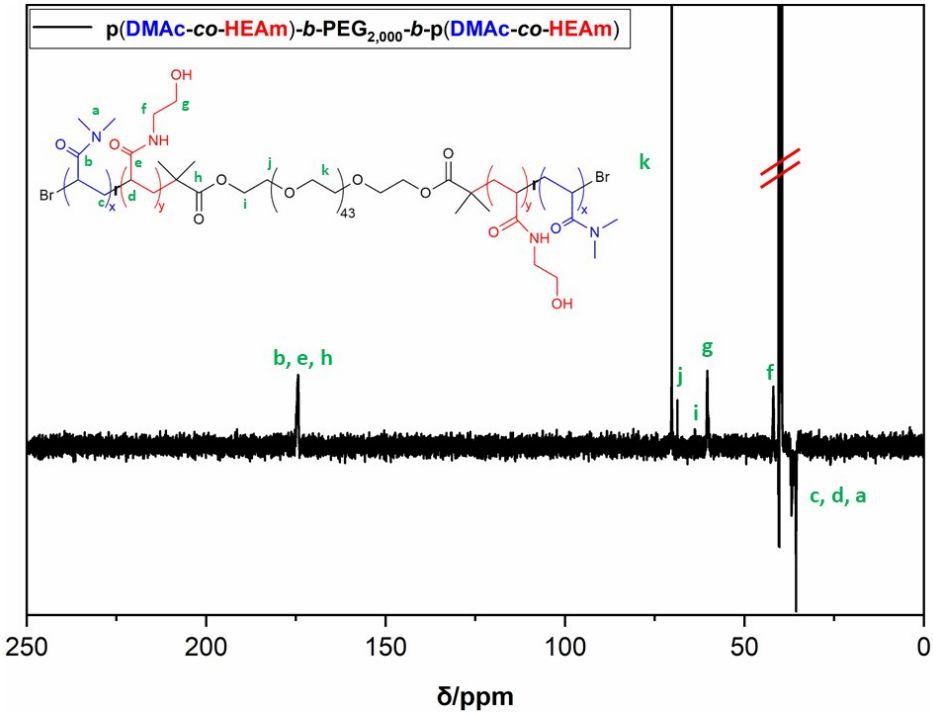

Figure S6. ^{13}C-NMR (400 MHz, DMSO-d$_6$) spectrum of p(DMAc$_x$-*co*-HEAm$_y$)-*b*-PEG$_{2,000}$-*b*-p(DMAc$_x$-*co*-HEAm$_y$) telechelic random copolymer.

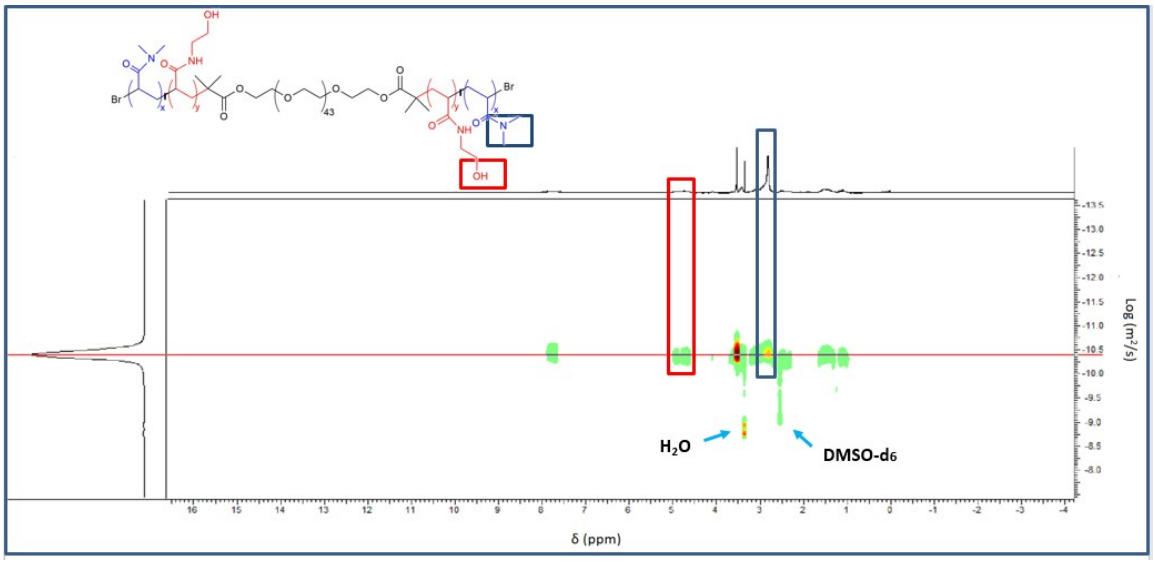

Figure S7. DOSY NMR (500 MHz, DMSO-d_6) spectrum of p(DMAc$_x$-*co*-HEAm$_y$)-*b*-PEG$_{2,000}$-*b*-p(DMAc$_x$-*co*-HEAm$_y$) telechelic random copolymer.

Supplementary data from the synthesis of the telechelic crosslinker p(DMAc$_x$-*co*-CHO$_y$)-*b*-PEG$_{2,000}$-*b*-p(DMAc$_x$-*co*-CHO$_y$)

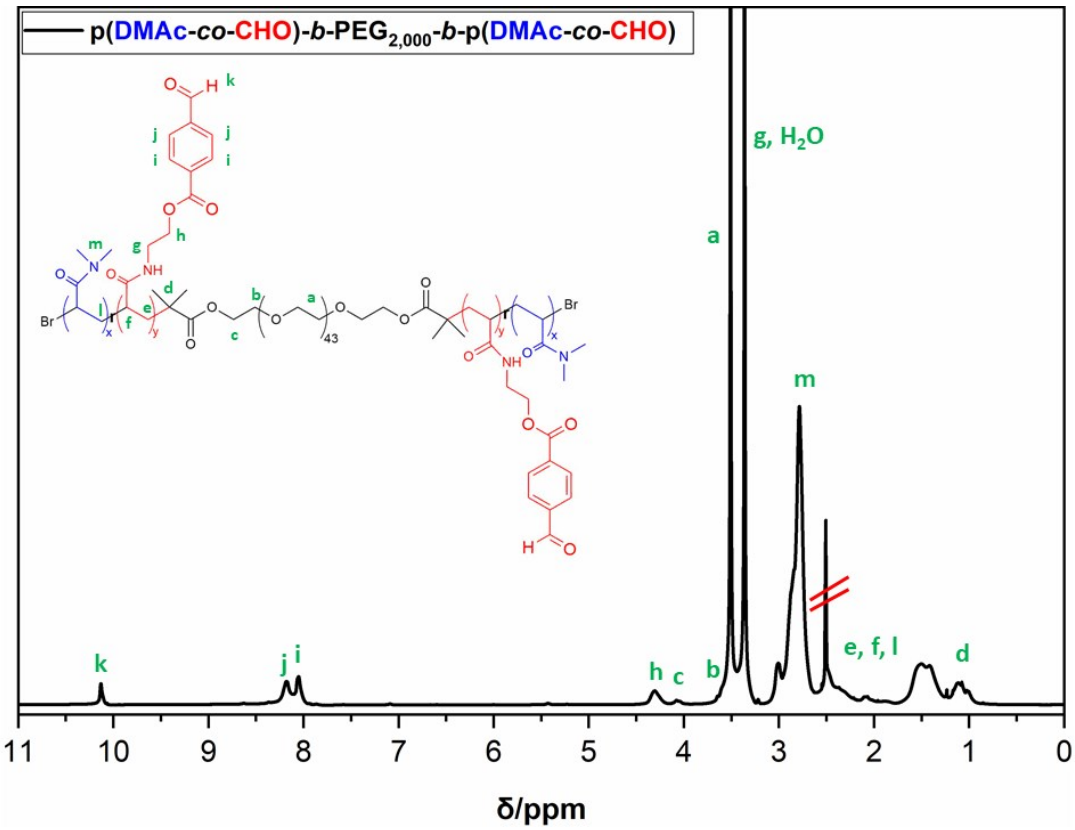

Figure S8. ^{1}H-NMR (500 MHz, DMSO-d_6) spectrum of p(DMAc$_x$-*co*-CHO$_y$)-*b*-PEG$_{2,000}$-*b*-p(DMAc$_x$-*co*-CHO$_y$) telechelic crosslinker.

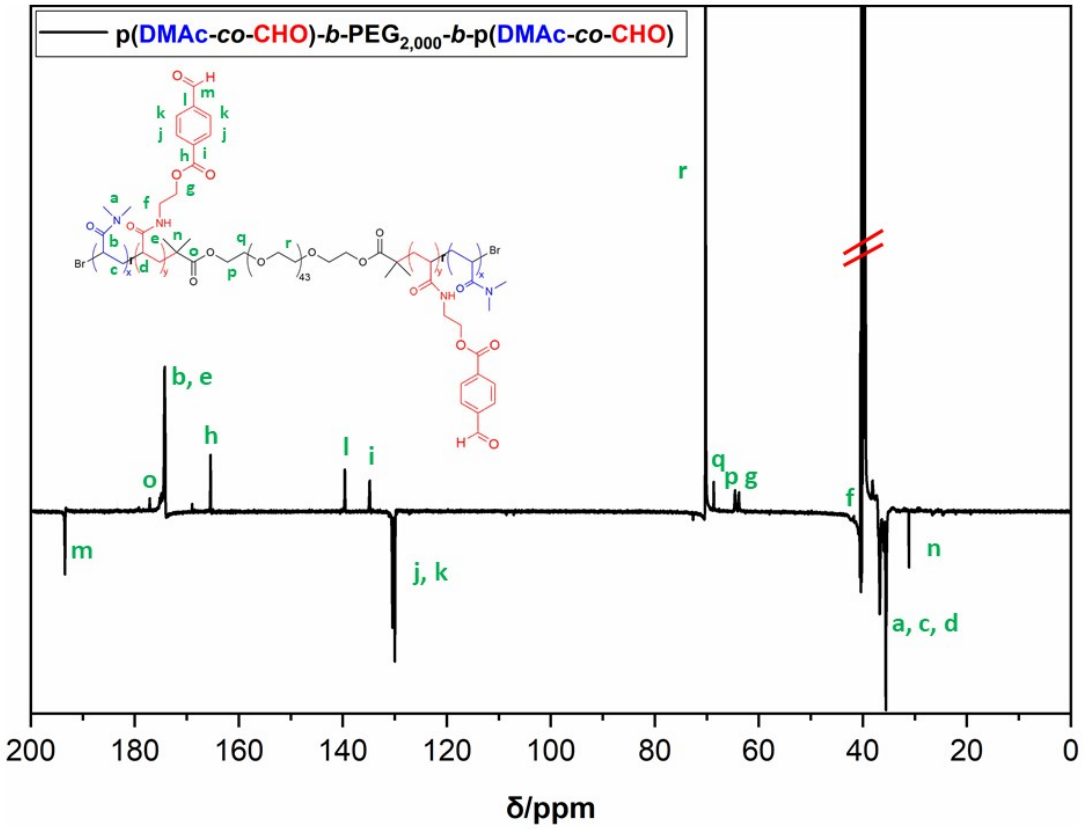

Figure S9. ^{13}C-NMR (500 MHz, DMSO-d_6) spectrum of p(DMAc$_x$-*co*-CHO$_y$)-*b*-PEG$_{2,000}$-*b*-p(DMAc$_x$-*co*-CHO$_y$) telechelic crosslinker.

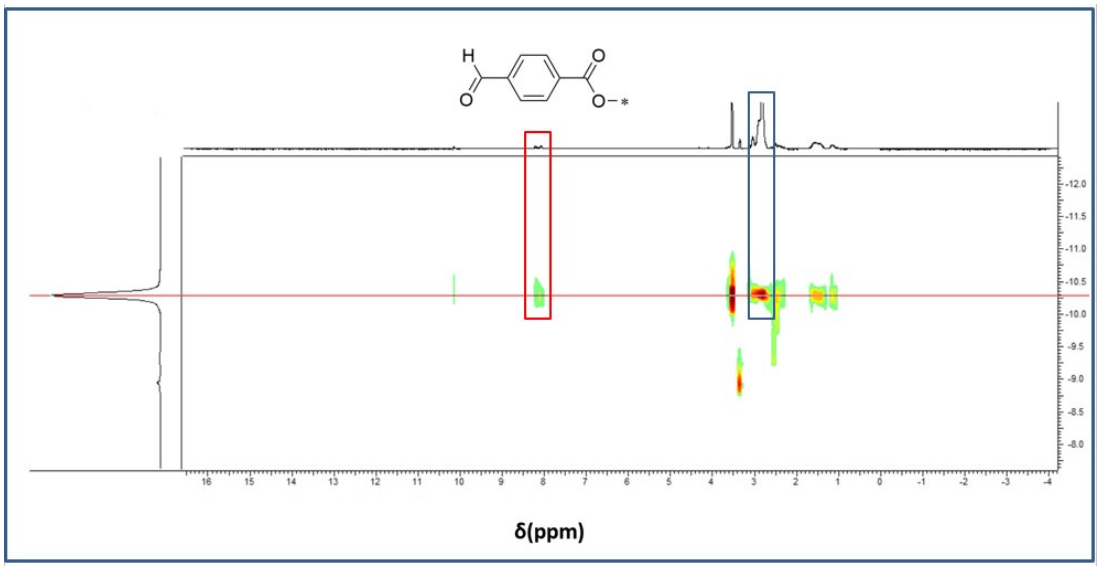

Figure S10. DOSY NMR (500 MHz, DMSO-d_6) spectrum of p(DMAc$_x$-*co*-CHO$_y$)-*b*-PEG$_{2,000}$-*b*-p(DMAc$_x$-*co*-CHO$_y$) telechelic crosslinker.

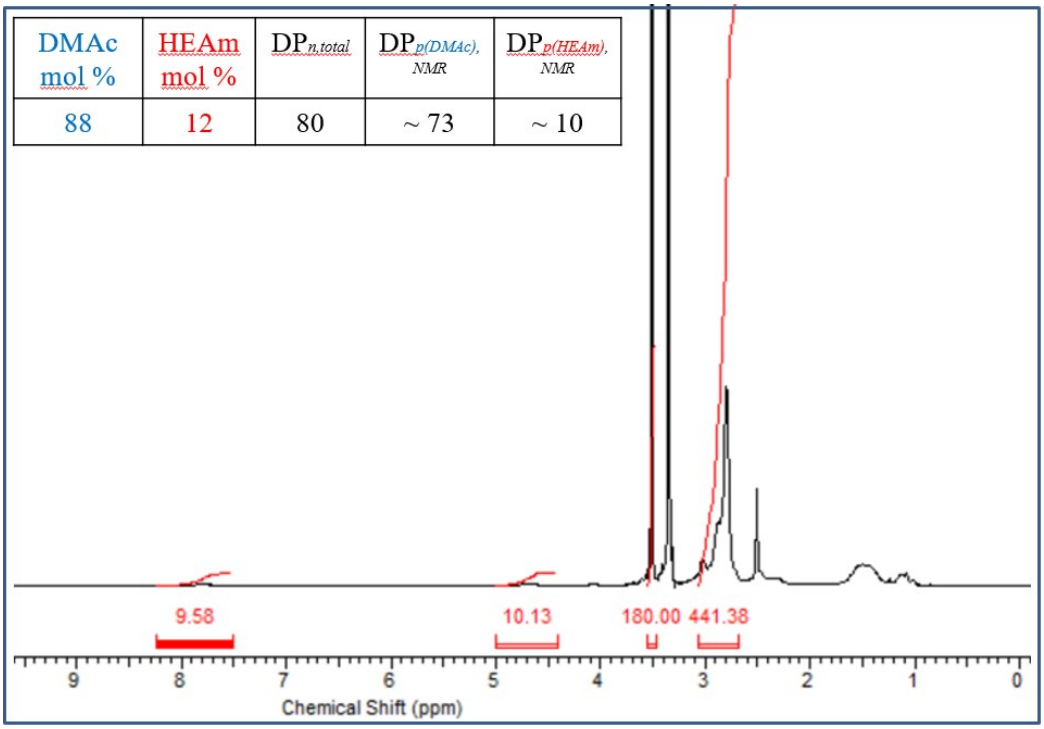

Figure S11. Integrated ^{1}H-NMR (500 MHz, DMSO-d_6) peaks of p(DMAc$_x$-*co*-HEAm$_y$)-*b*-PEG$_{2,000}$-*b*-p(DMAc$_x$-*co*-HEAm$_y$) telechelic copolymer at a molar ratio of (DMAc):(HEAm) = 88:12 with a targeted $DP_{n,total}$ = 80.

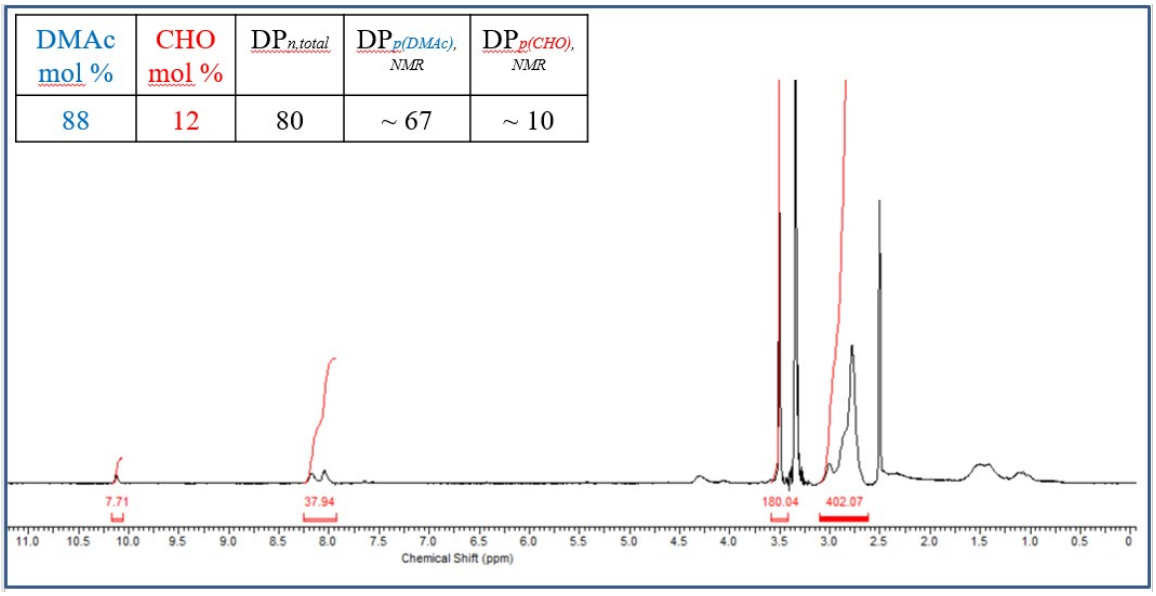

Figure S12. Integrated ^{1}H-NMR (500 MHz, DMSO-d_6) peaks of p(DMAc$_x$-*co*-CHO$_y$)-*b*-PEG$_{2,000}$-*b*-p(DMAc$_x$-*co*-CHO$_y$) telechelic crosslinker at a molar ratio of (DMAc):(HEAm) = 88:12 with a targeted $DP_{n,total}$ = 80.

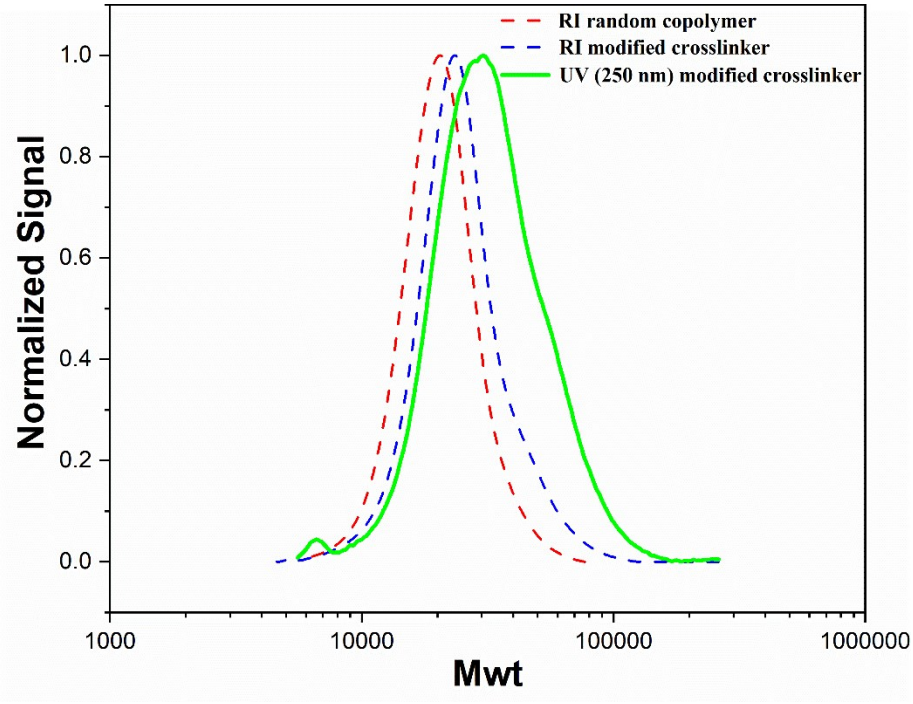

Figure S13. Combined RI and UV $_{(250\ nm)}$ traces of TXL crosslinker before and after post-modification as measured by DMF SEC using narrow PMMA calibration standards.

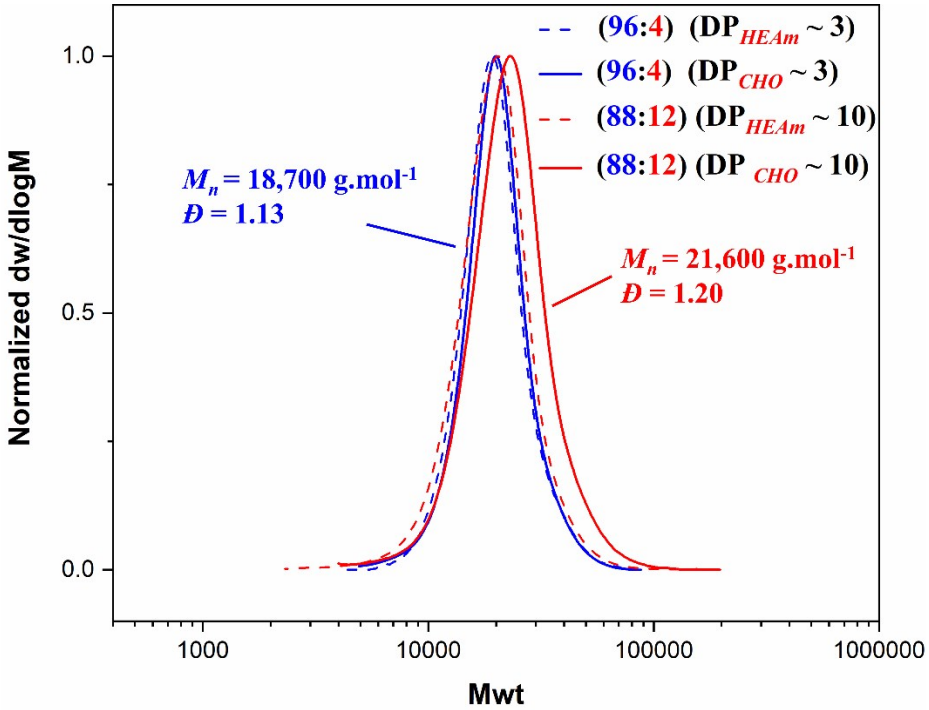

Figure S14. Molecular weight distribution RI traces of the copolymers used for the synthesis of TXL (red dashed) and TXL' (blue dashed) crosslinkers and of the TXL (red) and TXL'(blue) in DMF using PMMA narrow standards.

Table S2. Data from the synthesis of the telechelic copolymer via aqueous Cu-RDRP and its modification to crosslinker TXL'. For the Cu-RDRP polymerization, [I]:[Cu(I)]:[Me_6TREN] = [1]:[0.4]:[0.4] targeting a $DP_{n,total}$ = 80 at a molar ratio of DMAc to HEAm = 96:4

Entry	$M_{n,SEC}$ [a] (g.mol^{-1})	$M_{n,th}$ (g.mol^{-1})	$M_{n,NMR}$ (g.mol^{-1})	$Đ$	$DP_{p(DMAc),NMR}$	$DP_{p(HEAm),NMR}$	$DP_{p(CHO),NMR}$
Copolymer	18,300	9,900 [b]	9,980	1.13	~74	~3	-
TXL'	18,700	10,400 [b]	10,000	1.13	~70	-	~3

[a] Determined by SEC analysis in DMF compared to PMMA narrow molecular weight standards.

[b] Calculated for 95% conversion of DMAc and 97.5% conversion of HEAm

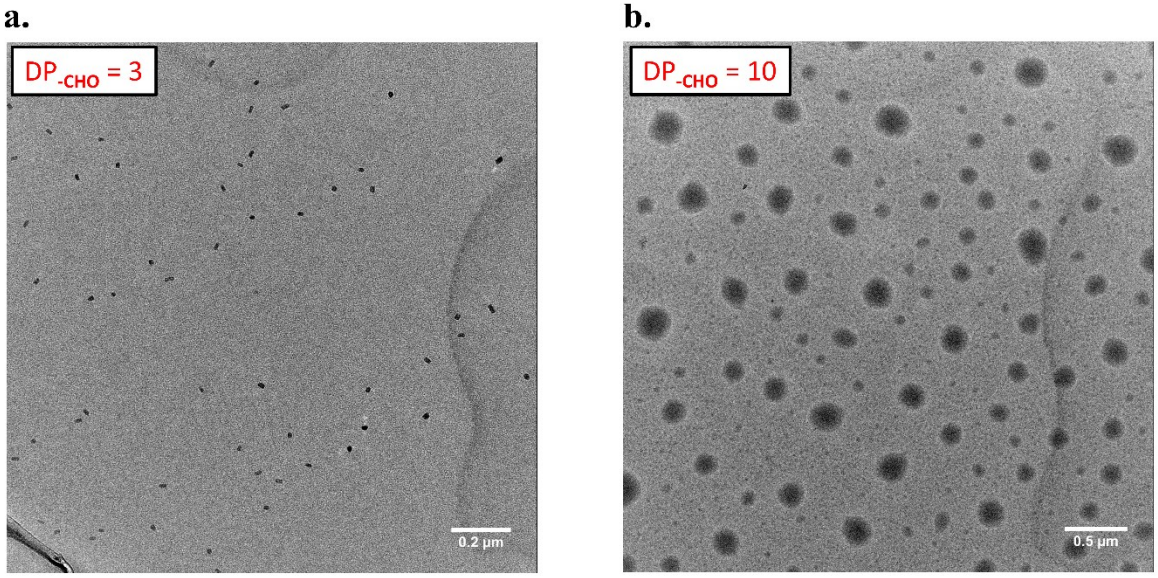

Figure S15. TEM images of TXL' (left) and TXL (right) crosslinkers from dispersed 5wt% solutions in water.

Supplementary data from Bi-PEG$_{4,000}$ bifunctional crosslinker synthesis and rheological characterization of GC/Bi-PEG$_{4,000}$ hydrogels

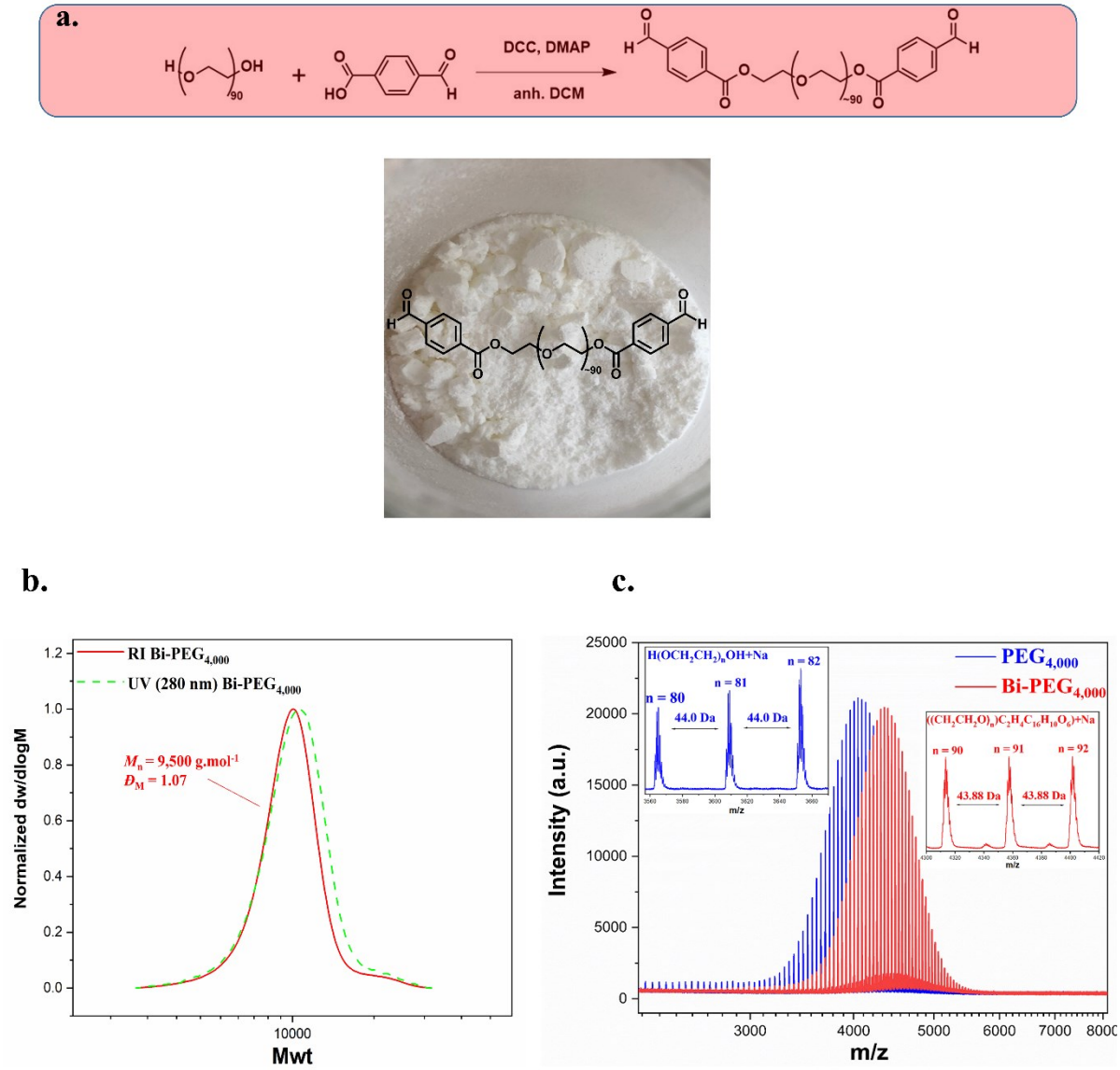

Figure S16. (a) Schematic of the synthesis of Bi-PEG$_{4,000}$ crosslinker. (b) Molecular weight distribution of synthesized Bi-PEG$_{4,000}$ crosslinker as measured by DMF SEC showing the RI and UV$_{(250\ nm)}$ signal. (c) MALDI-ToF spectra comparison of PEG$_{4,000}$ and Bi-PEG$_{4,000}$.

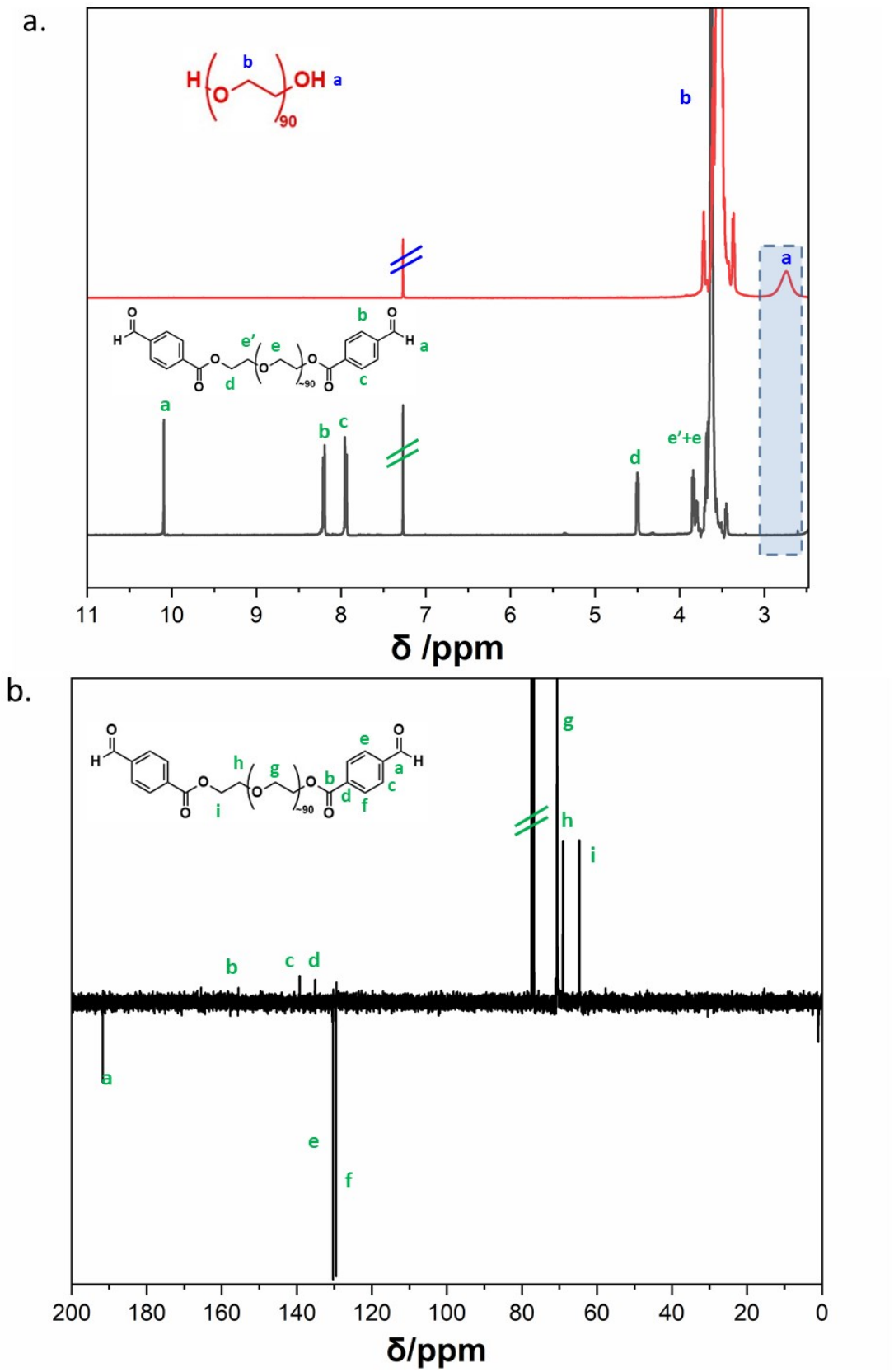

Figure S17. (a) ^{1}H-NMR (400 MHz, $CDCl_3$) spectrum of Bi-$PEG_{4,000}$ crosslinker. (b) . ^{13}C-NMR (400 MHz, $CDCl_3$) spectrum of Bi-$PEG_{4,000}$ crosslinker.

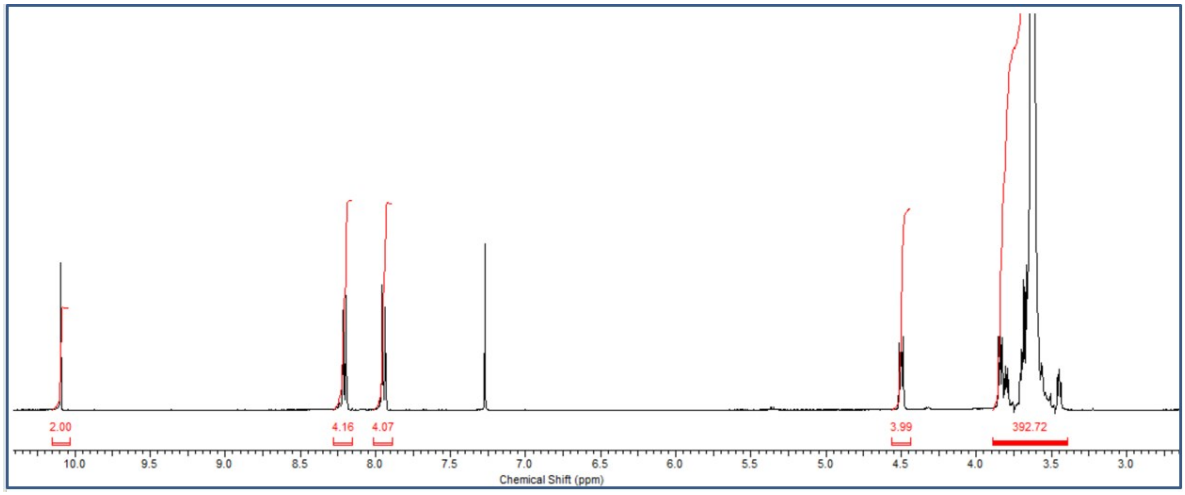

Figure S18. Integrated ^{1}H-NMR (400 MHz, $CDCl_3$) peaks of Bi-$PEG_{4,000}$ crosslinker proving the successful modification.

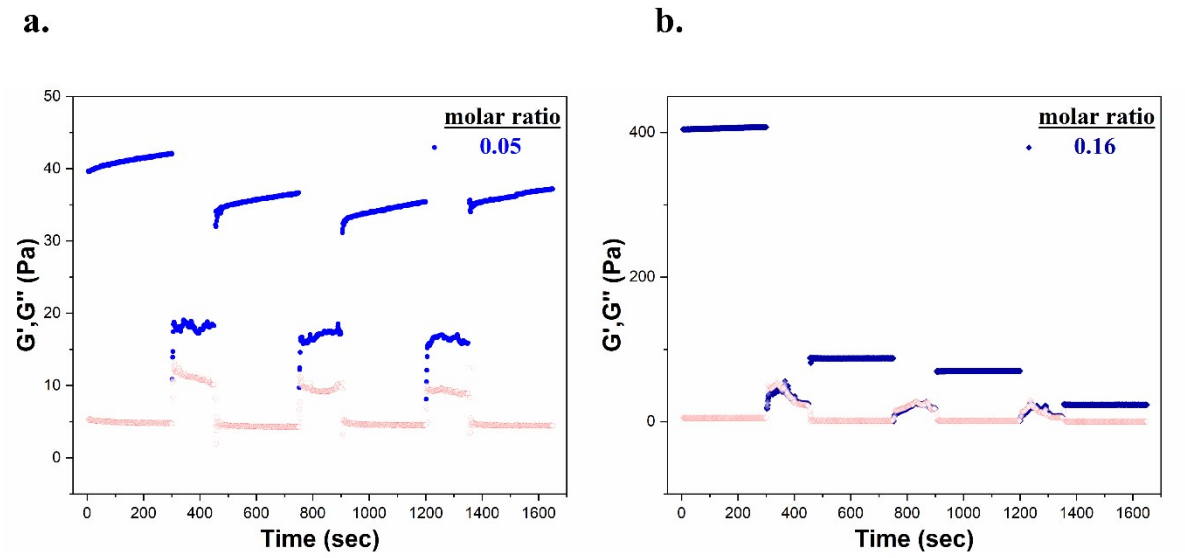

Figure S19. Alternate strain sweep experiments (between 1.0% and 350% at 25 ^{o}C) of GC/Bi-$PEG_{4,000}$ hydrogels at (a) 0.05 and (b) 0.16 molar ratio. In all occasions, storage modulus (G', filled symbols) and loss modulus (G'', fade symbols).

Kinetic data from the aqueous SET-LRP random copolymerization using a molar ratio of (DMAc:HEAm) = (88:12)

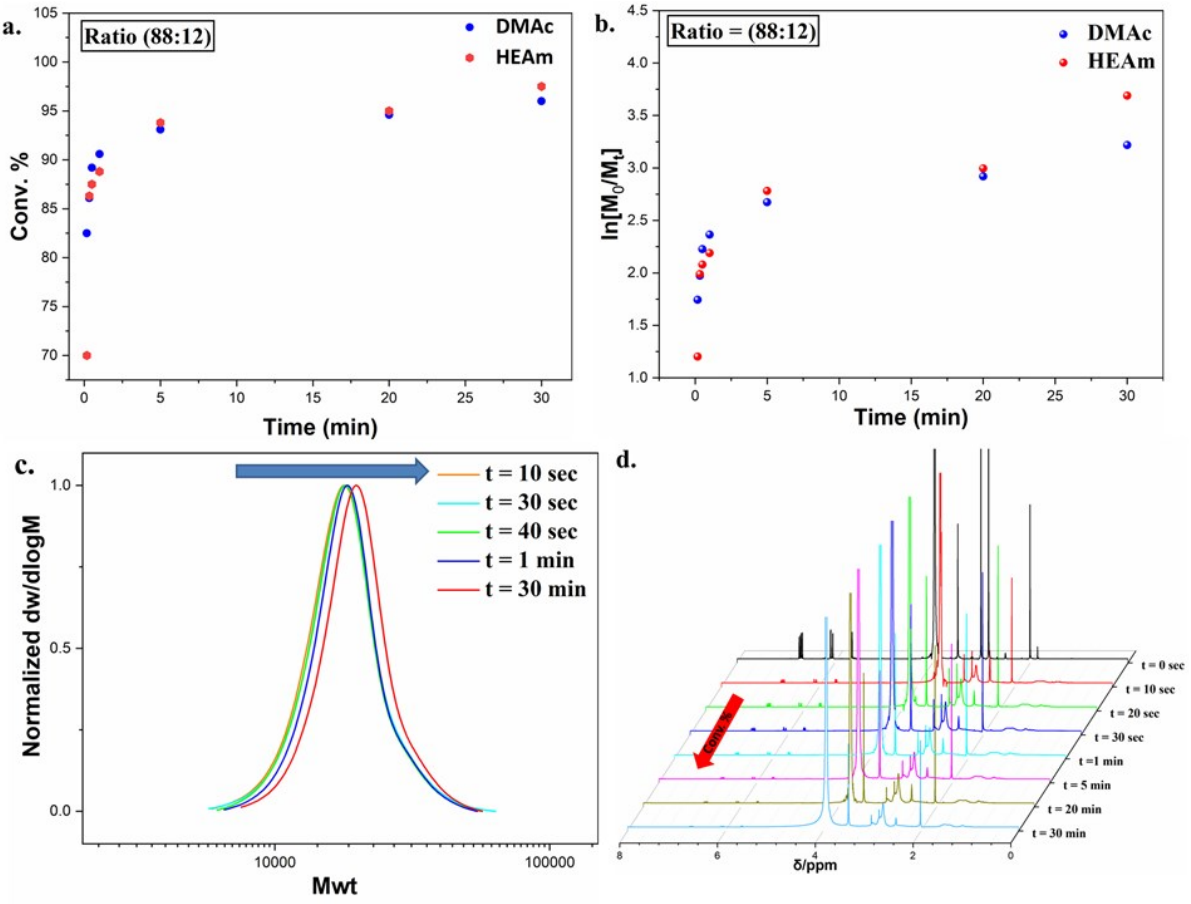

Figure S20. (a, b) Kinetic plots of conversion and $\ln[M_0]/[M_t]$ against time for both monomers (c) DMF SEC traces at different time intervals upon polymerization (d) Comparative ^{1}H-NMR (400 MHz, DMSO-d_6) spectra of the random copolymerization at various times using acetonitrile as an internal reference (δ = 2.07 ppm).

Ninhydrin assay data from the quantification of amine groups in commercial glycol chitosan

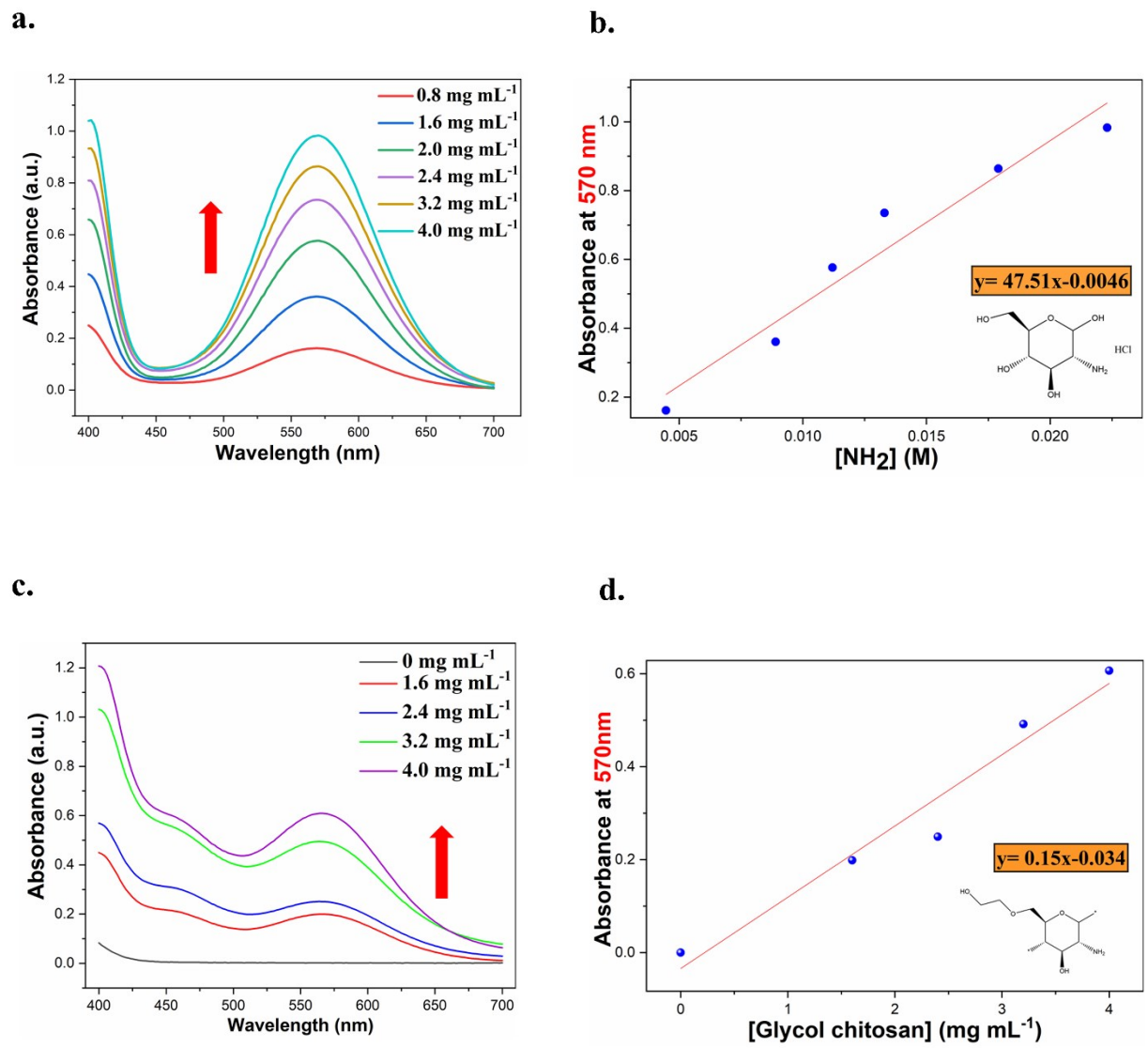

Figure S21. (a) UV-Vis absorption spectra of various concentrations of D-glucosamine in water (b) calibration graph of D-glucosamine based on UV-Vis absorption results at λ_{max} = 570 nm. (c) UV-Vis absorption spectra of various concentrations of glycol chitosan in water (d) calibration graph of glycol chitosan based on UV-Vis absorption results at λ_{max} = 570 nm.

Table S3. Results obtained from the calibration graphs of D-glucosamine and glycol chitosan using the ninhydrin assay.

Glycol chitosan (mg mL^{-1})	Abs (a.u.)	[NH_2] (mM)	mmol of NH_2/g of glycol chitosan
1.6	0.199	4.2	2.625
2.4	0.2497	5.3	2.208
3.2	0.492	10.4	3.25
4.0	0.607	12.8	3.2

Gelation kinetics of GC/TXL(x) hydrogels and self-healing tests

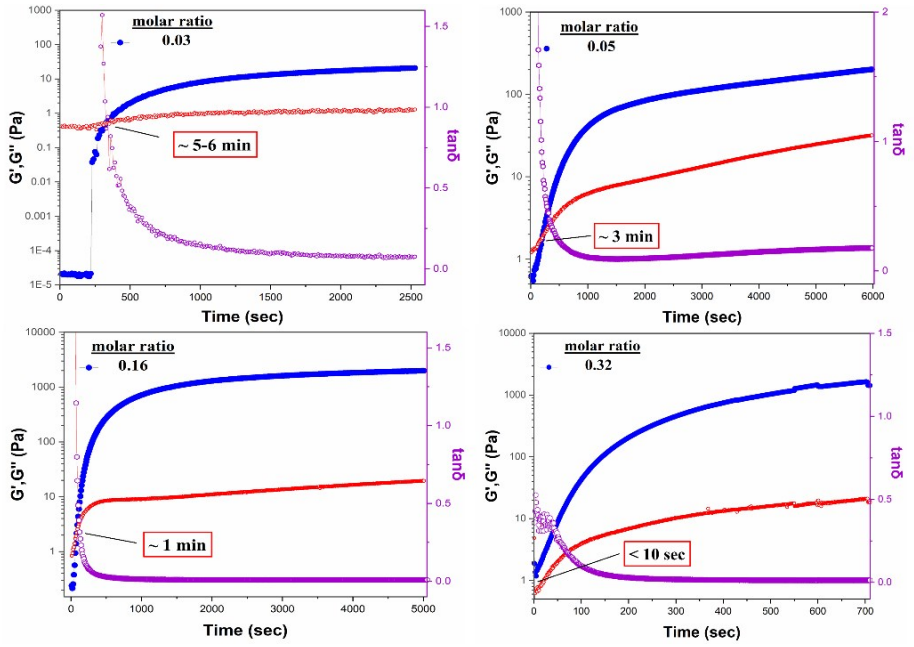

Figure S22. Gelation kinetics of GC/TXL hydrogels at 25 °C at four different molar ratios (-CHO/-NH_2): 0.03, 0.05, 0.16 and 0.32. G'(blue) and G'' (red).

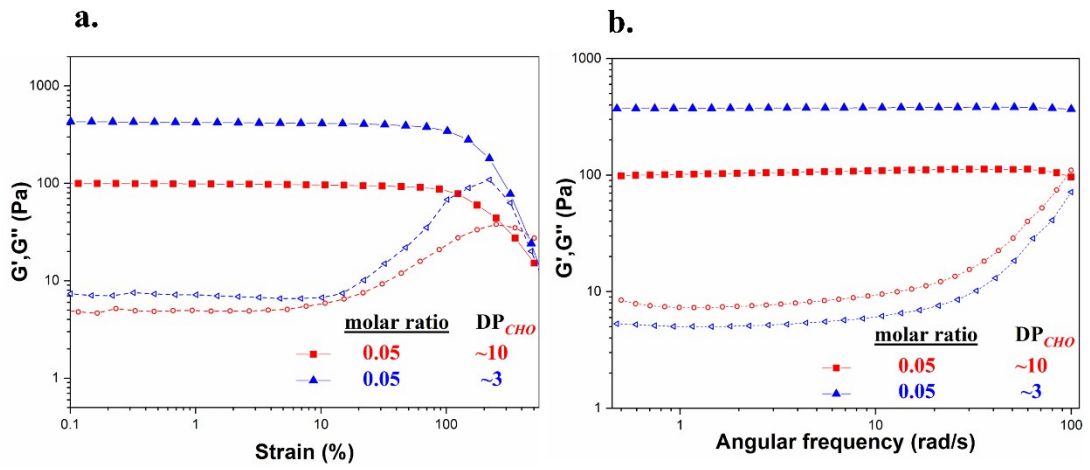

Figure S23. Rheological comparisons between GC/TXL(0.05) (red) and GC/TXL'(0.05) (blue) hydrogels (a) amplitude sweeps at 25 °C and at a constant frequency of $\omega = 10$ rad s^{-1} (b) frequency sweeps at 25 °C and at a constant strain of 5.0%. In all occasions, storage modulus (G', filled symbols) and loss modulus (G'', plane symbols).

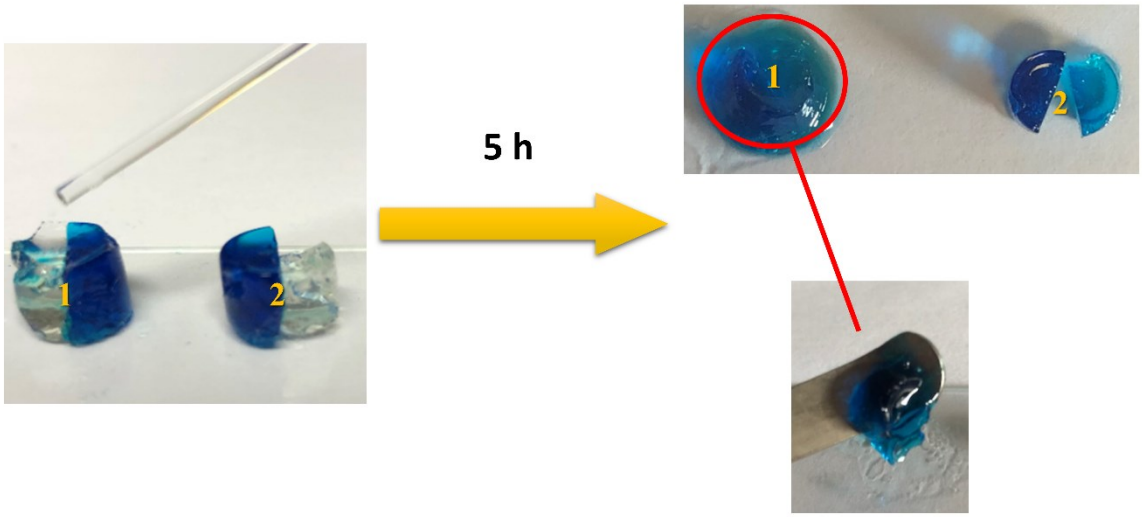

Figure S24. Self-healing comparisons of two GC/TXL**(0.05)** hydrogels after 5 h of addition of one drop of NaOH 10^{-4} M in gel 1. After 5 h, gel 1 self-healed while gel 2 showed no healing.

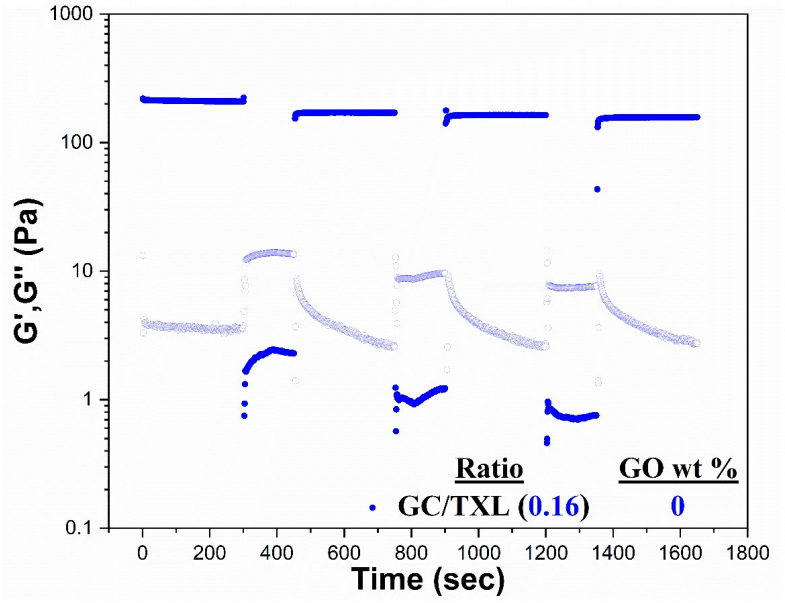

Figure S25. Alternate strain sweep experiments (between 1.0% and 350% at 25 °C) for GC/TXL**(0.16)** hydrogels where storage modulus (G', filled symbols) and loss modulus (G'', empty symbols).

Supplementary data from the GC/GO(y) nanosheets characterization

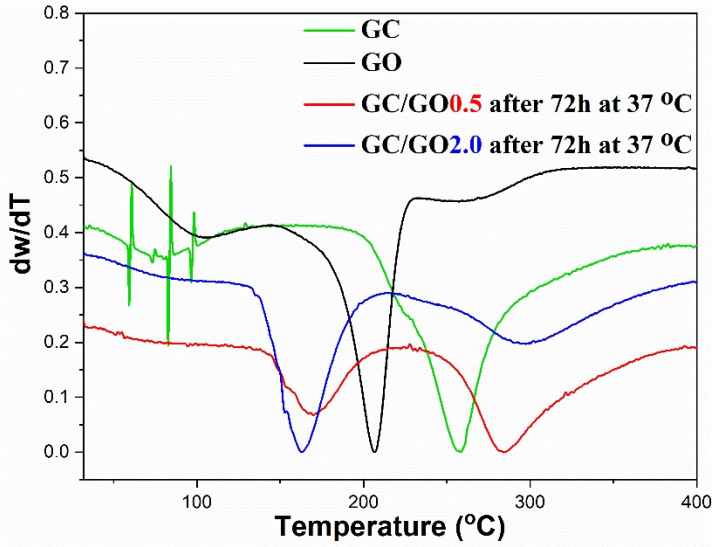

Figure S26. First derivative curves of GC/GO**(0.5)** and GC/GO**(2.0)** after 72 h at 37 °C, GO and GC.

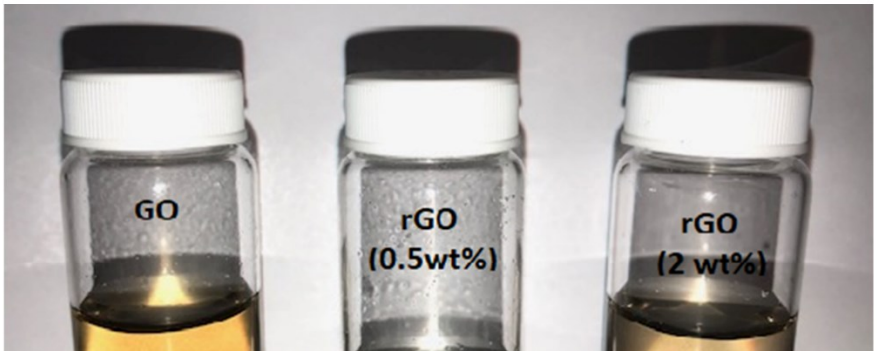

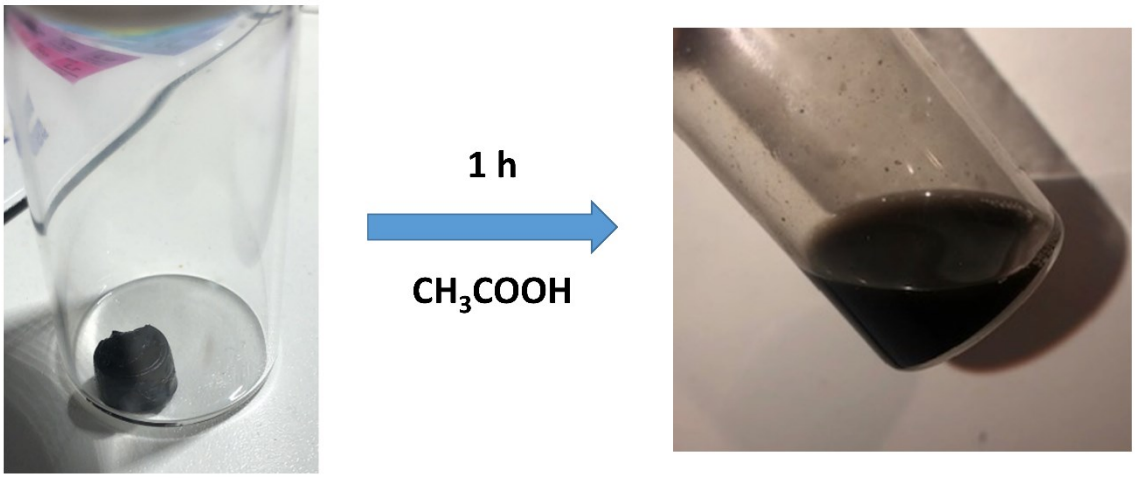

Figure S28. Dissolving GC/TXL**(x)**-GO**(y)** hydrogel in acetic acid (pH = 3) proving the formation of imine bonds.

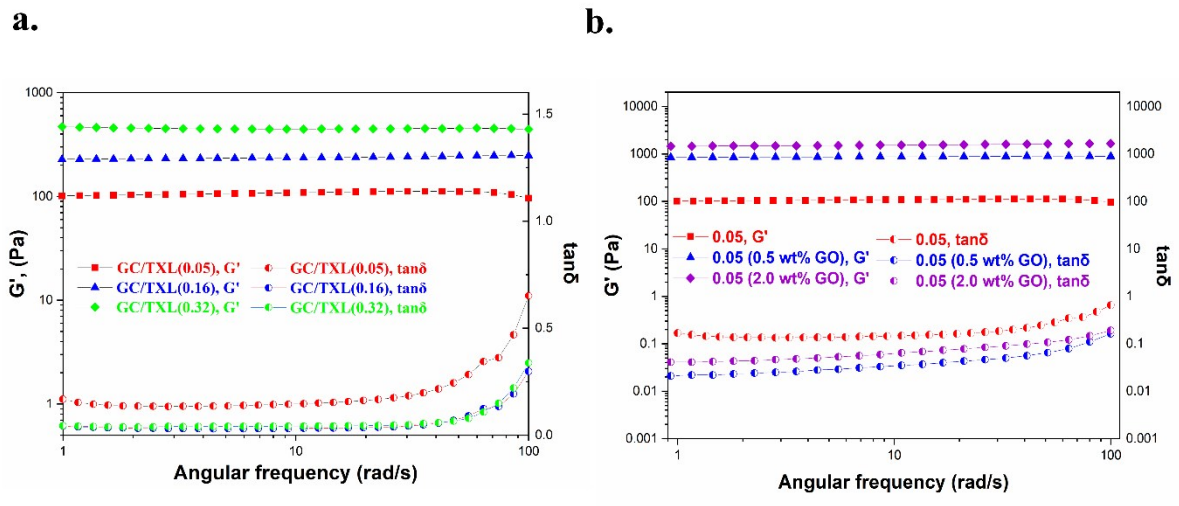

Figure S29. Frequency sweep experiments at 25 °C at a constant strain of 5.0% of (a) GC/TXL**(x)** and (b) GC/TXL**(0.05)**-GO**(y)** hydrogels showing the progress of the tanδ values by increasing frequency.

Compression data of dynamic hydrogel nanocomposites

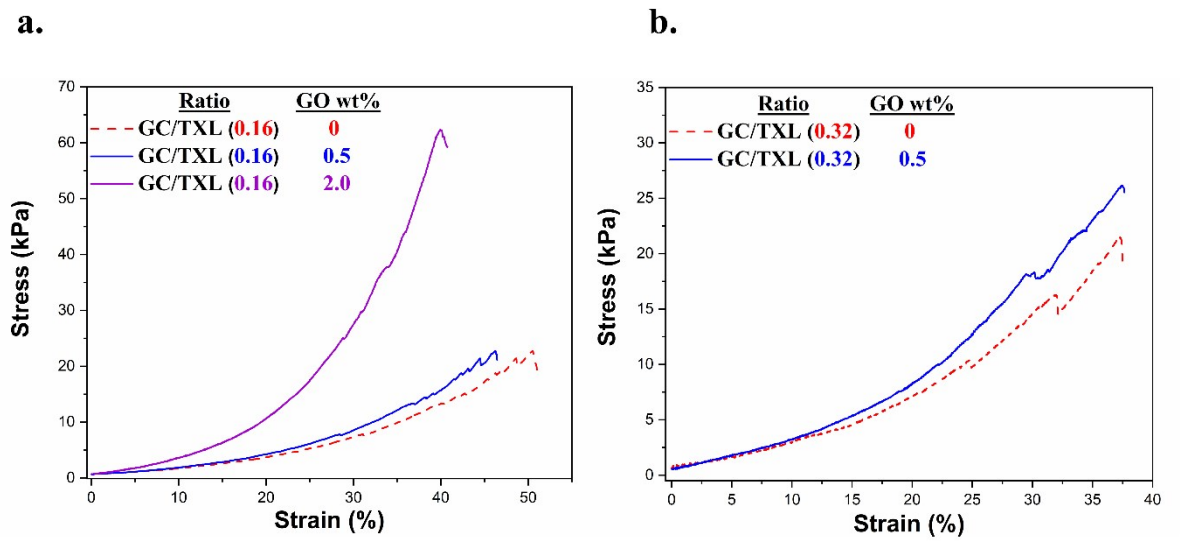

Figure S30. Representative compression tests on (a) GC/TXL**(0.16)** and (b) GC/TXL**(0.32)** hydrogels containing 0, 0.5 and 2.0 wt % of GO.

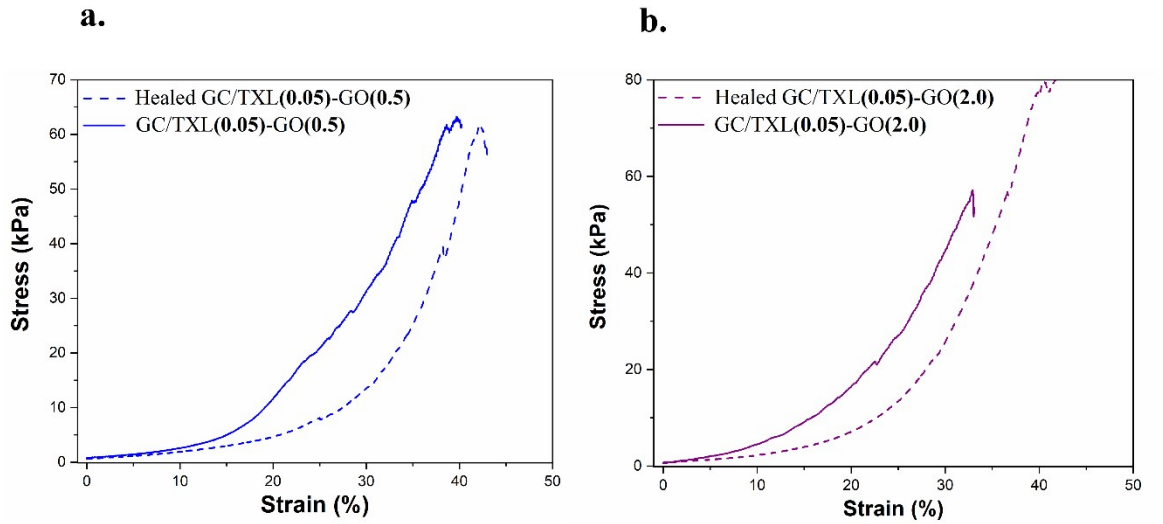

Figure S31. Representative compression test comparisons between self-healed and non self-healed gels reinforced with 0.5 and 2.0wt% GO gels.

Table S4. Tabulated uniaxial compression testing results of both pristine and GO reinforced hydrogels using

Molar ratio (-CHO/-NH_2)	GO (wt %)	Modulus (kPa) [a] (10% strain)	Strain at break (%)	Stress at break (kPa)	F_{max} (N)
0.05	0	23.0 ± 3.0	33.2 ± 5.4	32.9 ± 16.3	2.1 ± 0.9
0.05	0.5	35.0 ± 7.0	33.8 ± 3.5	44.8 ± 11.1	2.8 ± 0.7
0.05	2.0	48.7 ± 13.0	35.0 ± 2.8	55.6 ± 6.0	3.7 ± 0.4
0.16	0	19.9 ± 2.6	40.2 ± 4.6	28.7 ± 4.6	2.0 ± 0.3
0.16	0.5	28.9 ± 5.2	51.5 ± 5.4	41.4 ± 9.7	3.2 ± 0.5
0.16	2.0	38.8 ± 6.0	54.3 ± 2.3	58.1 ± 5.1	3.4 ± 0.5
0.32	0	27.7 ± 3.0	38.9 ± 3.8	20.9 ± 5.7	1.3 ± 0.3
0.32	0.5	31.7 ± 4.8	43.5 ± 6.0	21.9 ± 7.0	1.9 ± 0.6

crosslinker TXL.

[a] The compressive modulus was determined for the 10 % of the stress/strain curve.

Table S5. Tabulated uniaxial compression testing results of GO reinforced hydrogels before and after self-

Molar ratio (-CHO/-NH_2)	GO (wt %)	Modulus (kPa) [a] (10% strain)	Strain at break (%)	Stress at break (kPa)	SH (%)
0.05	0.5	35.0 ± 7.0	33.8 ± 3.5	44.8 ± 11.1	-
0.05	0.5	18.3 ± 0.5	43.1 ± 1.9	51.1 ± 7.6	52.3
0.05	2.0	48.7 ± 13.0	35.0 ± 2.8	55.6 ± 6.0	-
0.05	2.0	25.0 ± 5.4	45.2 ± 2.9	73.5 ± 6.4	51

healing using crosslinker TXL. The self-healed gels are highlighted with red.

[a] The compressive modulus was determined for the 10 % of the stress/strain curve.

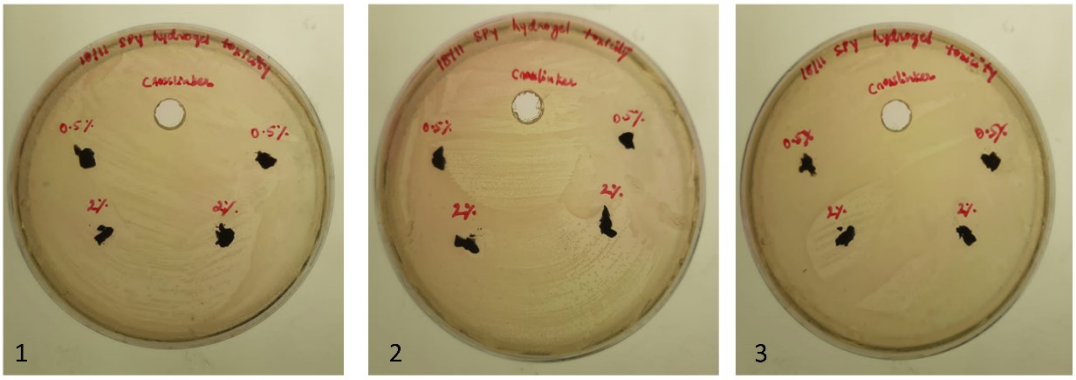

Figure S32. Disk diffusion assays of the nanocomposite hydrogels and crosslinker against *E. coli* 0.5%: GC/TXL**(0.05)**-GO**(0.5)**; 2%: GC/TXL**(0.05)**-GO**(2.0)**; Crosslinker: 5wt% solution of TXL crosslinker in PBS pH = 7.4.

1. M. Ciampolini and N. Nardi, *Inorg. Chem.*, 1966, **5**, 41-44.
2. E. Curotto and F. Aros, *Anal. Biochem.*, 1993, **211**, 240-241.